frontiers in CHEMISTRY

ORIGINAL RESEARCH ARTICLE
published: 24 December 2013
doi: 10.3389/fchem.2013.00038

Selectivity and self-diffusion of CO_2 and H_2 in a mixture on a graphite surface

Thuat T. Trinh[1], Thijs J. H. Vlugt[2], May-Britt Hägg[3], Dick Bedeaux[1] and Signe Kjelstrup[1,2]*

[1] Department of Chemistry, Norwegian University of Science and Technology, Trondheim, Norway
[2] Department of Process and Energy, Delft University of Technology, Delft, Netherlands
[3] Department of Chemical Engineering, Norwegian University of Science and Technology, Trondheim, Norway

Edited by:
Doo Soo Chung, Seoul National University, South Korea

Reviewed by:
Giancarlo Franzese, Universitat de Barcelona, Spain
Yun Hee Jang, Gwangju Institute of Science and Technology, South Korea

***Correspondence:**
Signe Kjelstrup, Department of Chemistry, Norwegian University of Science and Technology, Realfagbygget, Høgskoleringen 5, NO 7491 Trondheim, Norway
e-mail: signe.kjelstrup@ntnu.no

We performed classical molecular dynamics (MD) simulations to understand the mechanism of adsorption from a gas mixture of CO_2 and H_2 (mole fraction of $CO_2 = 0.30$) and diffusion along a graphite surface, with the aim to help enrich industrial off-gases in CO_2, separating out H_2. The temperature of the system in the simulation covered typical industrial conditions for off-gas treatment (250–550 K). The interaction energy of single molecules CO_2 or H_2 on graphite surface was calculated with classical force fields (FFs) and with Density Functional Theory (DFT). The results were in good agreement. The binding energy of CO_2 on graphite surface is three times larger than that of H_2. At lower temperatures, the selectivity of CO_2 over H_2 is five times larger than at higher temperatures. The position of the dividing surface was used to explain how the adsorption varies with pore size. In the temperature range studied, the self-diffusion coefficient of CO_2 is always smaller than of H_2. The temperature variation of the selectivities and the self-diffusion coefficient imply that the carbon molecular sieve membrane can be used for gas enrichment of CO_2.

Keywords: CO_2–H_2 mixture, adsorption, diffusion, molecular dynamics simulation, graphite

INTRODUCTION

The production of cheap membranes for CO_2 gas separation purposes is of primary importance for the realization of carbon capture and sequestration technologies (He et al., 2009; He and Hägg, 2011, 2012). One of the important applications of membranes is to separate CO_2 from a mixture of gases (Bernardo et al., 2009). Pressure swing adsorption (PSA) is one of the most common techniques to capture CO_2 from a mixture of CO_2 and H_2. This process requires large pressures, being different in the adsorption and desorption steps (Bernardo et al., 2009). In the adsorption step, CO_2 absorbs strongly into the carbon material at high pressure. Then in the later step, CO_2 desorbs at a much lower pressure. The energy costs depend on the manner this is performed; in one or more steps, with or without heat integrated. By using a molecular sieve membrane the separation can be performed as a continuous process, where the CO_2 is removed both by adsorption and diffusion from the high pressure side (feed side) to the low pressure side (permeate side). To provide an energy efficient design, we will need knowledge of molecular behavior, in particular of the selectivity and of transport properties at selected process conditions. Although there is a lot of recent progress in the modification of graphene material for adsorption and separation application of CO_2 and H_2 these material are not cheap (Kim et al., 2013; Li et al., 2013). Nano-porous, fibrous, carbonaceous materials are promising candidates from an economic point of view. In order to make further progress and produce molecular sieve membranes, better knowledge of several issues is needed. Central for membrane functionality are pore size, surface binding, surface wall transport, pore inlet control, carbon structure and composition. This work aims to provide such knowledge for a simplified, graphitic membrane, laying the grounds for more realistic future studies.

There are several experimental works and simulations devoted to understand adsorption of single component CO_2 and H_2 on carbon based material such as activated carbon and graphite (Guo et al., 2006; Haas et al., 2009; Levesque and Lamari, 2009; Jin et al., 2011; Saha et al., 2011). The experimentally obtained adsorption isotherm of CO_2 on active carbon is well-described by several models such as Langmuir (Jin et al., 2011), Tóth (Himeno et al., 2005), Dubinin-Astakhov (D-A) (Saha et al., 2011; Sevilla and Fuertes, 2012). Reported values for the enthalpy of adsorption depend on the type of adsorbent. Saha et al. reported that heats of adsorption of CO_2 in Maxsorb II and ACF (A-20) material are around -20 kJ/mol (Saha et al., 2011), while the untreated activated carbon C3345 material has a heat of adsorption -14 kJ/mol (Jin et al., 2011). Guo et al. reported that the heat of adsorption varied in the range -10 to -28 kJ/mol depending on the modification of the activated carbon material (Guo et al., 2006). Himeno et al. reported adsorption enthalpies in the range -16 to -25 kJ/mol for pure CO_2 on five different commercial activated carbons (Himeno et al., 2005).

Several simulation studies have given the adsorption isotherms for CO_2 on planar and pore-like graphite surfaces. Lim et al. (2010) reported data using a Langmuir adsorption model, and provided the self-diffusion coefficient ($D_s = 10^{-8} - 10^{-9}$ m^2/s) of CO_2 in a narrow pore (width 0.65–0.75 nm) for temperatures $T = 298 - 318$ K. Zhou et al. reported results for a wider range of pore sizes (0.7–3.4 nm) (Zhou and Wang, 2000). Their

values are comparable with those of Lim et al. The authors reported that CO_2 could form double layers. Both layers had a typical liquid-like structure (Zhou and Wang, 2000). Levesque et al. calculated the heat of CO_2 adsorption on activated carbon using Monte-Carlo simulations (Levesque and Lamari, 2009). The authors discussed how the adsorption enthalpy depended on the distribution of pore sizes.

Adsorption and diffusion of single component H_2 on graphite have recently been measured (Haas et al., 2009; Simon et al., 2010). The self-diffusion coefficient of H_2 on a graphite surface was found, using quasielastic neutron scattering (QENS) (Haas et al., 2009), to be in the range $10^{-6} - 10^{-7}$ m^2/s. Simulations found that pure H_2 on the graphite surface had a high lateral mobility (Simon et al., 2010).

Few computational results are reported on the selective adsorption of a mixture of CO_2 and H_2 on a graphite surface. Cao et al. described the graphite surface selectivity of the mixture at bulk compositions 50:50 and 20:80 at three different temperatures, slit pore sizes up to 3.0 nm and pressures up to 10 atm, using Monte Carlo simulations (Cao and Wu, 2005). The selectivity of CO_2 over H_2 depended on the pore size and the temperature. More recently, Kumar et al. (Vasanth Kumar and Rodríguez-Reinoso, 2012) reported results for CO_2/H_2 mixtures for molar ratios 10:90 and 20:80 on different graphite structures (nanotube, slit pores, or computer generated) at room temperature 298 K. It was shown that mixture separation was best with nanotubes. There are few studies on diffusion of CO_2 and H_2 on the graphite surface.

These studies give a motivation for the present work. We want to add to the knowledge of adsorption isotherms for a mixture CO_2 and H_2 at a typical syngas compositions (Rostrup-Nielsen and Christiansen, 2011) (mole fraction of $CO_2 = 0.30$) on a graphite surface, find the selectivity and self-diffusion coefficient for the components along the surface, and study these properties for a wide range of temperatures ($T = 250, 550$ K). Molecular dynamics (MD) simulations are well-suited to determine such properties. A snapshot of the gas mixture in equilibrium with the graphite is shown in **Figure 1**.

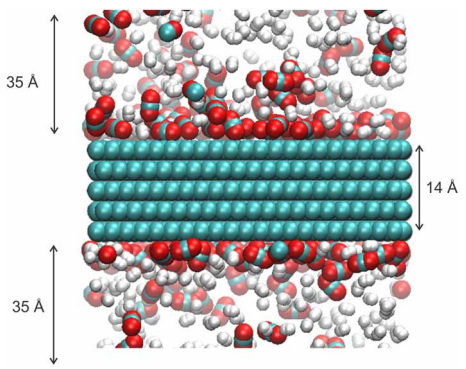

FIGURE 1 | Typical snapshot of the gas mixture of CO_2 and H_2 in equilibrium with a graphite surface. The temperature is $T = 300$ K and the number of particles is $N = 700$. The green, red, white are represented carbon, oxygen, and hydrogen atom, respectively.

MODEL

ISOTHERM ADSORPTION

The reaction between the gas phase and the adsorbed phase on the surface can be written for each component:

$$CO_2(\text{gas}) + \text{graphite} \rightleftharpoons CO_2(\text{graphite}) \quad (1)$$

$$H_2(\text{gas}) + \text{graphite} \rightleftharpoons H_2(\text{graphite}) \quad (2)$$

At equilibrium, the ideal gas chemical potential is equal to the surface chemical potential for each component:

$$\mu_g = \mu_s \quad (3)$$

$$\mu_g = \mu_g^0 + RT \ln\left(\frac{p}{p_0}\right) \quad (4)$$

where μ_g^0 is the standard chemical potential of the gas phase, i.e., the ideal chemical potential at the reference pressure p_0.

The chemical potential for the surface is

$$\mu_s = \mu_s^* + RT \ln\left(\gamma \frac{\Gamma}{\Gamma^*}\right) \quad (5)$$

where μ_s^* is the standard state chemical potential, γ is the activity coefficient, and Γ and Γ^* are the surface adsorption and standard surface adsorption, respectively. The surface adsorption is an excess quantity (see Equation 14 below for the definition).

SIMULATION DETAILS

To model the CO_2 adsorption and transport on the graphite surface, we performed classical MD simulations using the DL_POLY classic version 2.18 package (Smith et al., 2002). The system consisted of a graphite crystal and a mixture of CO_2 and H_2 molecules, ratio 30:70, an example of a syngas mixture (Rostrup-Nielsen and Christiansen, 2011). The graphite had hexagonal structure with P63/mmc without any defects. The graphite contained 4284 carbon atoms and was constructed from 5 sheets of graphene which represented the property of graphite well (Boukhvalov et al., 2008). We oriented the graphene sheets in our simulation box such that the surfaces of the sheets were perpendicular to the z direction. The size of the simulation box was $42 \times 51 \times 84$Å^3. In the z direction, the system covers a pore size of 70 Å and a graphite width of 14 Å (**Figure 1**). Periodic boundary conditions are used in all directions. At least 10 systems with different total number (N) of molecules, where $10 < N < 7.0$ were simulated. For each N, simulations were performed at 8 different temperatures in the range 250–550 K.

The MD simulation had time steps of 1fs. The initial configuration was constructed by randomly distributing the CO_2/H_2 mixture over the graphite surface. The system was stabilized during 1000 ps by *NVT* runs with the Nosé-Hoover thermostat (Martyna et al., 1992). When the system was in the thermal equilibrium, we performed another 1000 ps run with microcanonical ensemble conditions (*NVE*) to study adsorption and transport properties. The average values of temperature and pressure in *NVE* simulation were within 1% of expected values. In total 2×10^6 MD steps was performed and this is sufficiently long to

get good statistics and consistent trajectories. Each trajectory was printed every 100 time step and stored for further analysis.

POTENTIAL ENERGY INTERACTION

We fixed the graphite layer and used the rigid body model of Transferable Potentials for Phase Equilibria (TraPPE) for CO_2 and H_2 molecule. This potential can describe well the vapor-liquid and the liquid-solid equilibria of CO_2 (Potoff and Siepmann, 2001). The intermolecular potential contained long range Coulombic interactions, and a shifted and truncated 12-6 Lennard-Jones (LJ) potential (Allen and Tildesley, 1989).

$$V_{ij}^{nb} = V_{ij}^{\mathrm{LJ}} + V_{ij}^{\mathrm{coulombic}} \tag{6}$$

$$V_{ij}(r_{ij}) = 4\varepsilon_{ij}\left[\left(\frac{\sigma_{ij}}{r_{ij}}\right)^{12} - \left(\frac{\sigma_{ij}}{r_{ij}}\right)^{6}\right] \tag{7}$$

$$V_{ij}^{\mathrm{LJ}}(r_{ij}) = \begin{cases} V_{ij}(r_{ij}) - V_{ij}(r_c) & r_{ij} < r_c \\ 0 & r_{ij} > r_c \end{cases} \tag{8}$$

where r_{ij} is the distance between atoms i and j, ε_{ij}, and σ_{ij} are LJ potential parameters, and r_c is the cutoff radius. The LJ interaction parameters between the different types of atoms were calculated from the Lorentz-Berthlot mixing rules (Allen and Tildesley, 1989)

$$\varepsilon_{ij} = \sqrt{\varepsilon_{ii}\varepsilon_{jj}} \tag{9}$$

$$\sigma_{ij} = \frac{1}{2}\left(\sigma_{ii} + \sigma_{jj}\right) \tag{10}$$

The Coulombic interactions were:

$$V_{ij}^{\mathrm{coulombic}} = \frac{1}{4\pi\varepsilon_0}\frac{q_i q_j}{r_{ij}} \tag{11}$$

where q_i, q_j are the charges on atoms i, j, and ε_0 is the dielectric constant. In our work, we use the Smoothed Particle Mesh Ewald technique implemented in the DL_POLY package for the electrostatic interactions, see Essmann et al. (1995) for more details. The parameters, taken from the DREIDING (Mayo et al., 1990) and TraPPE (Potoff and Siepmann, 2001) force fields (FFs), are listed in **Table 1**.

DENSITY FUNCTIONAL THEORY (DFT) CALCULATIONS

To evaluate the results using classical FFs, we also performed DFT to calculate the binding energy of CO_2 and H_2 on graphite surface. For the *ab-initio* simulations, DFT optimization and single energy were performed using Quickstep (Vandevondele et al., 2005) which is part of the CP2K program package (http://cp2k.berlios.de, 2011). Quickstep employs the Gaussian and plane waves (GPW) method (Lippert et al., 1997) which makes efficient and accurate density-functional calculations of large systems possible. We used the Goedecker-Teter-Hutter (GTH) pseudopotentials (Goedecker et al., 1996; Hartwigsen et al., 1998) to describe atomic cores and the PBE exchange-correlation functional (Perdew et al., 1996). One-electron wave functions were developed under the DZVP-MOLOPT (DZPM) basis set, offering a double-zeta valence complemented with polarization functions (Vandevondele and Hutter, 2007). An energy cut-off of 400 Ry was selected for the additional plane wave basis sets. To describe the van der Waals interactions, an empirical dispersion correction of Grimme's type was applied (Grimme, 2006).

DFT is a computationally expensive method for a large system. Hence we used a much smaller model than with the FF method. Five sheets of 32 carbon atom each was used to construct the graphite surface. The graphite geometry was chosen similarly to the FF simulation. The system was fully optimized, and then CO_2 and H_2 molecules were fixed at selected distance from the surface for single point energy calculations.

We used the DFT method to calculate the interaction energy between each component (CO_2, H_2) and graphite surface.

$$E_{\mathrm{CO_2}}^{i} = E_{\mathrm{Graphite-CO_2}} - (E_{\mathrm{Graphite}} + E_{\mathrm{CO_2}}) \tag{12}$$

$$E_{\mathrm{H_2}}^{i} = E_{\mathrm{Graphite-H_2}} - (E_{\mathrm{Graphite}} + E_{\mathrm{H_2}}) \tag{13}$$

For X = CO_2 or H_2:E_X^i, $E_{\mathrm{Graphite}-X}$, E_{Graphite}, E_X are the interaction energy, potential energy of graphite-X system, potential energy of graphite and potential energy of X, respectively.

The optimum distance of adsorption is the distance between molecule and graphite surface where the interaction energy profile has a minimum.

Table 1 | Interaction potential parameters used in simulation.

Atom	σ (Å)	ε /k_B (K)	charge (*e*)
C (in CO_2)	2.80	27	0.7
O (in CO_2)	3.05	79	–0.35
C (graphite)	3.34	26	0
H (in H_2)	2.64	28	0

RESULTS AND DISCUSSION

INTERACTIONS BETWEEN CO_2/H_2 AND THE GRAPHITE SURFACE

Figure 2 shows the adsorption energy profile of a single CO_2 or H_2 molecule on the graphite surface calculated with the FF and DFT methods for the optimum molecule-surface distance. This distance and the adsorption energy are given in **Table 2** for both methods. CO_2 is favorably adsorbed at the bridge site and is parallel to the surface, while H_2 prefers the hollow site and is perpendicular to the surface. Our finding is supported by Rubes et al. (2010). The profiles of the plots in **Figure 2** are very similar, meaning that the FF results can be seen as a good representation of the DFT calculations. The values of the interaction energy of CO_2 and H_2 on the surface (**Table 2**) are typical for physisorption. For CO_2 on surface, the interaction energy $E_{\mathrm{CO_2}}^{i} = -15$ and -17 kJ/mol for FF and DFT, respectively. The optimum distance of CO_2 and surface is around 3.20–3.30 Å (**Table 2**). The interaction energy in the case of H_2 on the surface is smaller than in the case of CO_2 on the surface ($E_{\mathrm{H_2}}^{i} = -6$ and -5 kJ/mol for FF and DFT, compare **Figures 2B** to **2A**) while the optimum distance of H_2 and the surface is around 3.0 Å (**Figure 2B**). Furthermore, the interaction energies are in good agreement with other DFT calculations (Montoya et al., 2003; Rubes et al., 2010), meaning that our results for binding energies and distances are robust.

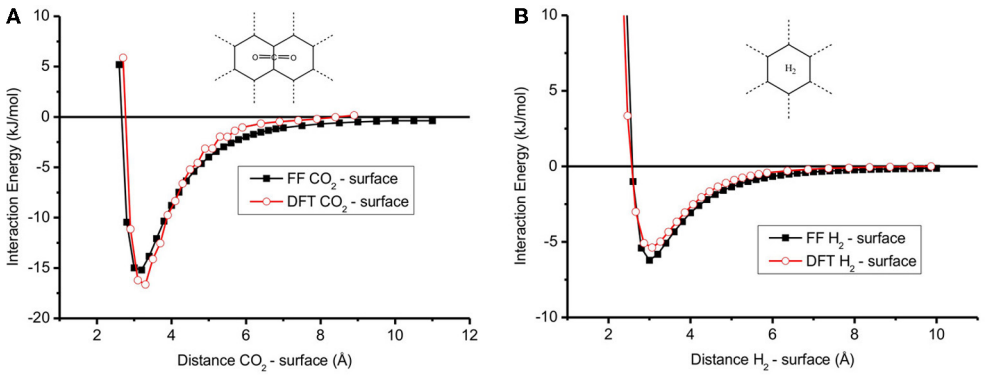

FIGURE 2 | Interaction energy between (A) CO_2—graphite surface and (B) H_2—graphite surface calculated with DFT and Force Field method. The result of FF method is comparable with DFT method.

Table 2 | Optimum distance for adsorption and corresponding interaction energies for the FF and DFT methods used.

Method	Force field	DFT PBE-D, periodic
Optimum distance CO_2 – surface	3.20 Å	3.30 Å
Interaction energy CO_2 – surface $E^i_{CO_2}$	−15 kJ/mol	−17 kJ/mol
Optimum distance H_2 – surface	3.0 Å	3.0 Å
Interaction energy H_2 – surface $E^i_{H_2}$	−6 kJ/mol	−5 kJ/mol

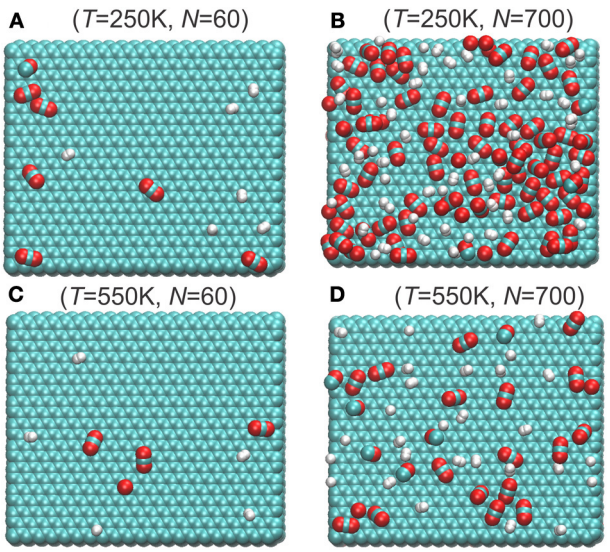

FIGURE 3 | Typical snaphosts of top view of molecules adsorbed on the graphite surface at different temperatures and total number of particles (A) $T = 250$ K, $N = 60$; (B) $T = 250$ K, $N = 700$; (C) $T = 550$ K, $N = 60$; (D) $T = 550$ K, $N = 700$, cf. Figure 6. Only the adsorbed layers below the dividing surface are shown (cf. Equation 14). The green, red, white represent carbon, oxygen, and hydrogen atoms, respectively.

THE STRUCTURE OF MIXTURE ON SURFACE

Typical snapshots of mixtures adsorbed on graphite surfaces at different temperatures and total number of particles are depicted in **Figure 3**. With the same number of total molecules, there are more molecules adsorbed on the surface at lower temperature (compare **Figures 3A,B**) than at higher temperatures (Compare **Figures 3C,D**). The ratio CO_2/H_2 on the graphite surface is also larger in the low temperature range than at high temperatures. H_2 and CO_2 appears randomly distributed on the surface when surface has low loading (**Figures 3A–C**). But when the surface has high loading and CO_2 is preferred at the surface, the H_2 molecules seem to occupy the voids between the CO_2 molecules (**Figure 3D**).

SURFACE EXCESS DENSITIES

In the thermodynamic description, we use the surface excess concentration (adsorption) Γ, as defined originally by Gibbs, see Kjelstrup and Bedeaux (2008) for a detailed description. The interface is defined as the thin layer between phases where densities deviate from the densities in the adjacent phases. We restrict ourselves to surfaces parallel to the graphite surface, so

$$\Gamma = \int_0^\infty \left(C(z) - C^{\text{gas}}(\alpha)\theta(z-\alpha)\right) dz \qquad (14)$$

where Γ is the adsorption, and C, C^{gas} are the total concentration of molecules and the concentration in the gas, respectively (**Figure 4**). The Heaviside function, θ, is by definition unity, when the argument is positive, and zero when argument is negative. The extension of the surface can differ from molecule to molecule, as illustrated for the two molecules in question in **Figure 4**, and a choice must be made. The positions α_{H_2} and α_{CO_2} are defined as the positions where the concentrations of H_2 and CO_2 are 5% above the bulk value. For the CO_2/H_2 mixture, we choose the dividing surface $\alpha = \alpha_{CO_2}$ as given in the figure for the integral in Equation (14). Adsorption isotherms (**Figures 6, 7** below) were obtained by plotting the surface excess concentration provided by Equation (14) for both components using this position, vs. the gas pressure. The gas pressures of CO_2 and H_2 were obtained by

separate calculations where the simulation box contained only CO_2 or H_2 at different temperatures and concentrations. The total gas pressure is the sum of partial pressure of CO_2 and H_2.

The distributions of CO_2 and H_2 molecules perpendicular to the surface, have two peaks, see **Figure 4**. The first peak of CO_2 is located around 3.2 Å and the first of H_2 is located around 3.0 Å. These peaks correspond to the optimum distances of adsorption of the gas molecules as described in the previous section. The radial distribution functions (RDF) of CO_2–H_2 and CO_2–CO_2 molecules of the different layers across the surface are reported in **Figure 5**. The RDF of CO_2–CO_2 in the adsorbed phase has a liquid-like behavior and this agrees with other simulations of pure CO_2 on graphite surface (Zhou and Wang, 2000). The RDF of CO_2–CO_2 in the gas phase is less ordered, showing a homogenous behavior. The positions of maximum RDF of the adsorbed layers and the gas of CO_2 are comparable. The RDF of CO_2–H_2 has a typical gas-like behavior, which indicates that CO_2–H_2 is near an ideal mixture. The interactions between the gas components are not as important as the interactions between the gas and the graphite surface.

THE ADSORPTION ON A GRAPHITE SURFACE

The adsorption of CO_2 and H_2 at different temperatures are presented in **Figure 6**. When the temperature increases, the adsorption decreases, as expected. This behavior was also observed with CO_2/H_2 mixtures of molar ratios (20:80 and 10:90) on a different carbon pore structure, using Monte Carlo simulations (Vasanth Kumar and Rodríguez-Reinoso, 2012). The adsorption of hydrogen, Γ_{H_2}, is much lower than the value of Γ_{CO_2}. We explain the preference of CO_2 to H_2 on the surface by its stronger interaction with graphite (**Table 2**). The H_2 adsorbs less than CO_2 and prefers the gas phase. The total adsorption of both CO_2 and H_2 is shown in **Figure 7**. When the temperature increases the mixture adsorbs less.

Separation of mixtures

The separation ratio S (selectivity) of CO_2/H_2 mixture is defined as:

$$S = \frac{n\mathrm{CO_2(adsorbed)}}{n\mathrm{CO_2(gas)}} \times \frac{n\mathrm{H_2(gas)}}{n\mathrm{H_2(adsorbed)}} \qquad (15)$$

The selectivity is commonly used to define the efficiency of a (membrane) material to separate CO_2 from a mixture of CO_2, H_2. For activated carbon, S depends on the mixture composition and on the pore sizes (Vasanth Kumar and Rodríguez-Reinoso, 2012). Our surface model can be seen as a graphite crystal with an extra-large slit pore, of 7 nm diameter. The results obtained for S are presented in **Figure 8**. At low pressures (<25 atm), the accuracy in S is small (within ±30%) because the small number of molecules leads to poor statistics. At higher pressures (>25 atm), the values of S vary around a constant average value within ±10% for each temperature.

Monte Carlo simulations by Kumar et al. (Vasanth Kumar and Rodríguez-Reinoso, 2012) showed that the selectivity increases with increasing pressure with a slit pore geometry. Cao et al. (Cao and Wu, 2005) reported that the selectivity of CO_2 over H_2 size decreased when the pressure increased in the low pressure region, using Monte Carlo simulations. The results of Cao et al. can be understood from the selectivity of CO_2 over H_2 being maximum for carbon pores around 15 Å (Cao and Wu, 2005), being the double of the surface extension shown in **Figure 4**. The number of molecules adsorbed larger, relatively speaking, for pore sizes below 2α, leading to high selectivities for such pores or pore distributions. By finding the extension of the surface, one can thus decide on the optimal pore size of the material.

The data in **Figure 8** show that the selectivity is essentially invariant of the pressure for pressures above 25 atm. The results

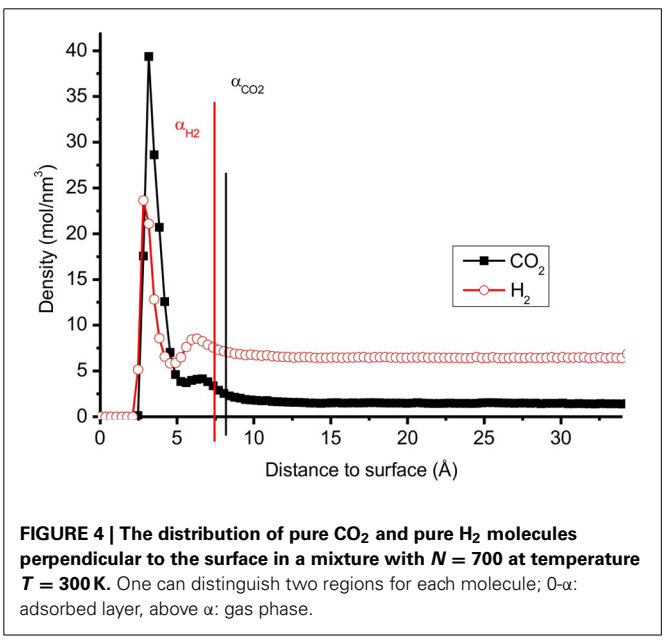

FIGURE 4 | The distribution of pure CO_2 and pure H_2 molecules perpendicular to the surface in a mixture with $N = 700$ at temperature $T = 300$ K. One can distinguish two regions for each molecule; 0-α: adsorbed layer, above α: gas phase.

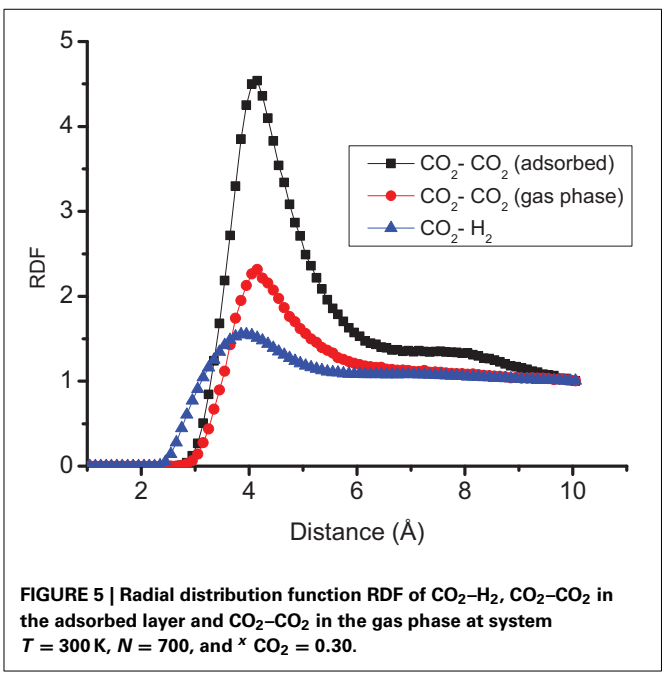

FIGURE 5 | Radial distribution function RDF of CO_2–H_2, CO_2–CO_2 in the adsorbed layer and CO_2–CO_2 in the gas phase at system $T = 300$ K, $N = 700$, and ^{x} $CO_2 = 0.30$.

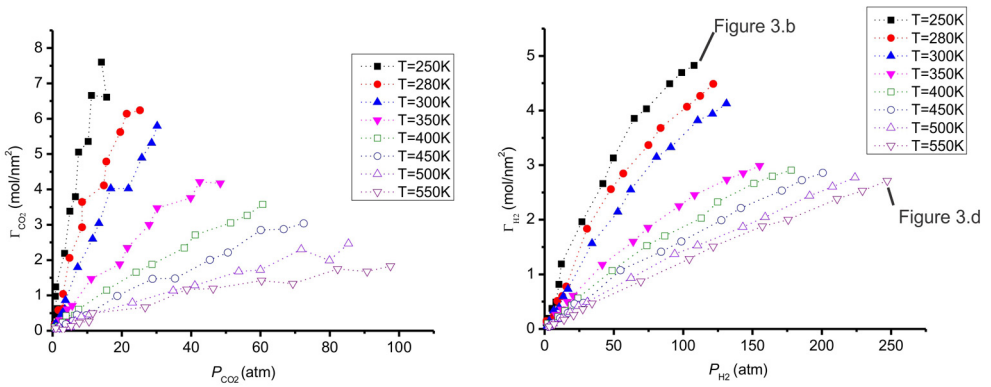

FIGURE 6 | The adsorption of CO_2 and H_2 as a function of partial pressure of CO_2 (left) and H_2 (right) at different temperatures. The states used for the snapshots in **Figures 3B,D** are shown.

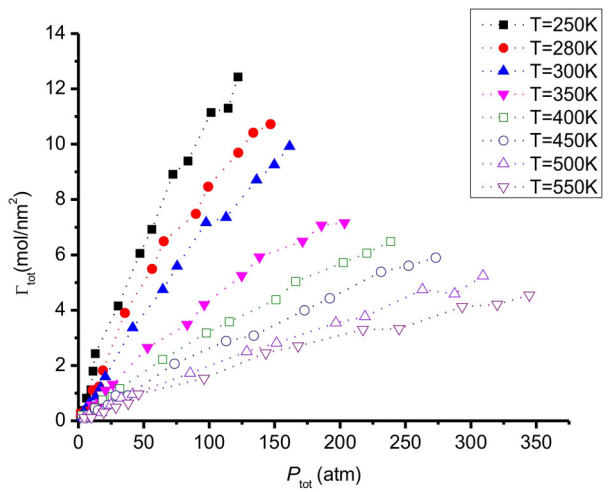

FIGURE 7 | Total amount of CO_2/H_2 adsorbed on a graphite surface as a function of gas pressure at different temperatures.

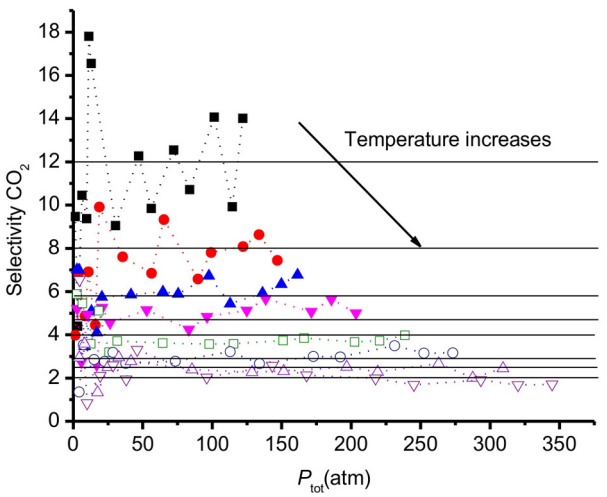

FIGURE 8 | Selectivity of CO_2 relative to H_2 *vs.* the total pressure of the system. Results refer to a graphite surface with pore size 7 nm at different temperatures from 250 to 550 K. The selectivity decreases with increasing temperatures.

indicate that the selectivity goes down below 25 atm. All values S are in the range 2–18 and decreases when the temperature increases. At 250K, the average selectivity is 12. At the highest temperature, 550 K, S reduces to the average value 2. At high temperatures the two gases have similar adsorption behavior, CO_2 does not adsorb much stronger than H_2. This changes at lower temperatures. The trend of S is in good agreement with other simulations of CO_2/H_2 mixtures in slit pores with smaller pore sizes, using the GCMC technique (Cao and Wu, 2005).

SURFACE SELF-DIFFUSION

The self-diffusion of CO_2 and H_2 along the surface was studied. The self-diffusion coefficient of molecule was obtained from:

$$D_{||}^{s} = \lim_{t\to\infty}\left[\frac{1}{2dNt}\sum_{i=1}^{N}\left\langle|r_i(t) - r_i(0)|^2\right\rangle\right] \quad (16)$$

where d is the dimensionality (for surface $d = 2$), N is the total molecules, $r_i(t)$ and $r_i(0)$ are the projections of the position of molecules on the surface at time t and time 0.

All molecules were included in the mean-squared displacement calculations as described in previous studies (Haas et al., 2009). By plotting the logarithm of the diffusion coefficients found vs. the inverse of temperature, we obtained an Arrhenius plot. This was used to estimate the temperature dependence of the diffusion coefficient according to

$$D(T) = D_0 \exp\left(\frac{-E^{act}}{RT}\right) \quad (17)$$

where D_0 is the pre-exponential factor, R is the gas constant, and $Eact$ is the activation energy.

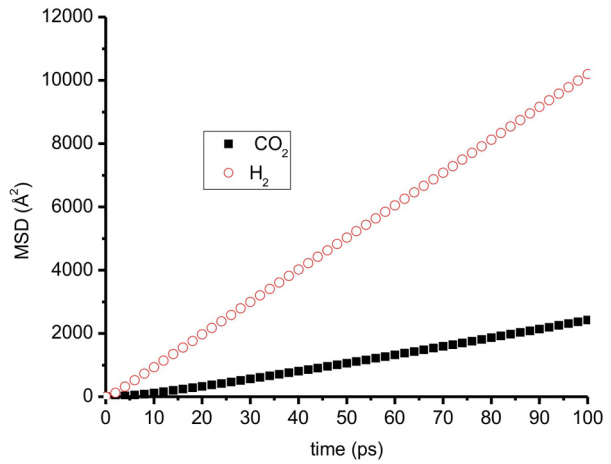

FIGURE 9 | The mean-squared displacement (MSD) of CO_2 and H_2 on a graphite surface at $T = 300$ K, $N = 700$, mole fraction of $CO_2 = 0.3$ H_2 has much higher MSD than CO_2.

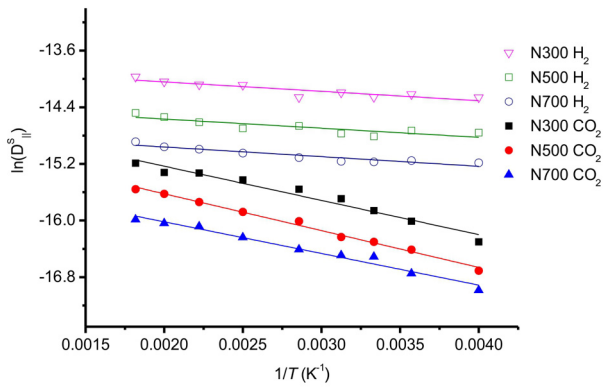

FIGURE 10 | Natural logarithm of the self-diffusion coefficients as a function of the inverse temperature of selected system.

Table 3 | Summary of results on self-diffusion parameters cf. Equation (17) for a mixture of CO_2 and H_2 on a graphite surface.

	This work (simulation) on graphite surface	References
$D^0_{CO_2}$	2.7×10^{-7}–6.4×10^{-6} (m^2/s)	MD simulation (Zhou and Wang, 2000; Lim et al., 2010) (very small slit pore <1 nm) $\sim 1 \times 10^{-9}$ (m^2/s)
$E^{act}_{CO_2}$	3.5–4.3 kJ/mol	(very small slit pore <1 nm) 5.77–6.08 kJ/mol ref (Lim et al., 2010)
$D^0_{H_2}$	4.2×10^{-7}–1.1×10^{-6} (m^2/s)	QENS experiment (Haas et al., 2009) (graphite surface) 1.9×10^{-7} (m^2/s) for 1 ML 3.5×10^{-7} (m^2/s) for 0.5 ML
$E^{act}_{H_2}$	1.0–1.2 kJ/mol	QENS experiment (Haas et al., 2009) (graphite surface) 1.0–1.1 (kJ/mol)

Figure 9 shows an example of mean-squared displacement of CO_2 and H_2 parallel to the graphite surface at temperature 300 K. It is clearly shown that H_2 diffuses much faster than CO_2. We observe a similar trend for all cases: H_2 always has a higher self-diffusion coefficient than CO_2, because H_2 is lighter than CO_2.

The activation barrier for self-diffusion was obtained by calculating the slope of the linear relationship between the natural logarithm of the self-diffusion coefficient and $1/T$ (**Figure 10**). We found that activation barriers for self-diffusion of CO_2 varying in the range $E^{act}_{CO_2} = 3.5$–4.3 kJ/mol. These values are smaller than the values reported by Lim et al. (2010), giving energy barriers in the range 5.77–6.08 kJ/mol for CO_2 diffusion. The pores were smaller than 1.0 nm in this case, however. The self-diffusion coefficient of CO_2 along the graphite surface is higher than values obtained from simulations with smaller pore sizes (<1 nm) (Zhou and Wang, 2000; Lim et al., 2010). This is because larger pores allow surface CO_2 more space to diffuse, and less interaction between CO_2 and carbon atoms of graphite. Under the conditions used here with pore size ~7 nm, CO_2 will diffuse relatively faster and with a smaller diffusion barrier than inside a 1 nm slit pore. This adds to the knowledge on CO_2 diffusion on graphite surfaces.

For H_2 on graphite surface, we found self-diffusion barriers in the range $E^{act}_{H_2} = 1.0$–1.1 kJ/mol. The self-diffusion barrier for H_2 is good agreement with experimental data for H_2 transport on graphite surface. QENS gave 1.0–1.2 kJ/mol, Haas et al. (2009). The $D^0_{H_2}$ in our study was also in a very good agreement with other experimental values (**Table 3**).

The diffusion coefficient of H_2 is larger than that of CO_2 (**Figure 11**). The barrier to self-diffusion of CO_2 is four times larger than that of H_2 on a graphite surface. The CO_2 diffusion depends much more on the temperature than that of H_2. Hence at high temperature, CO_2, and H_2 will have similar diffusion coefficients.

The results (**Figure 8**) have shown that the selectivity is more or less invariant to the total pressure above 25 atm, but highly dependent on the temperature. The permeation of a gas through a membrane is a product of diffusion and adsorption, and the main driving force for separation is given by the partial pressure difference over the membrane. This means that separation of CO_2 from a mixture with H_2 at any pressure can best occur at low temperatures, when graphite as an adsorbing material is most effective for CO_2. The adsorbed CO_2 will then induce pore size reduction, hence hindering H_2 to permeate, and hence CO_2 can be selectively permeated. At high temperature, the permeated gas will be enriched in H_2 since adsorbed CO_2 will no longer be blocking the pores, and there will hardly be any selectivity between the two. However, if the pore size can be tailored to the range of 3–4 Å, one may achieve a diffusional selectivity in favor of H_2 at high temperatures (**Figure 10**).

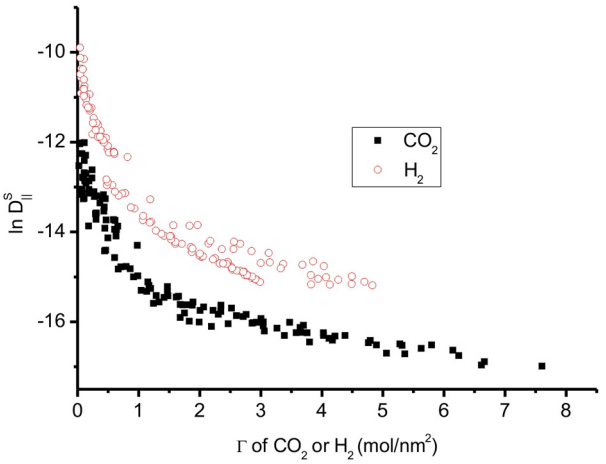

FIGURE 11 | Natural logarithm of all self-diffusion coefficients *vs.* adsorption of CO_2 and H_2. H_2 has higher diffusion coefficients than CO_2.

The PSA process is based on adsorption at high pressures and desorption at low pressures. By combining PSA with low-high temperature (TSA-process), further enrichment of CO_2 could be obtained by repeating these equilibrium adsorption steps on activated carbon. By modifying the structure of a graphite surface, one may enhance the separation of CO_2 out of mixture with H_2; both when considering a PSA-TSA process as well as for carbon molecular sieve membranes.

CONCLUSION

In this work, we have used Equilibrium MD to study the adsorption, selectivity, and self-diffusion of a mixture of CO_2 and H_2 (overall mole fraction 0.30 of CO_2) adsorbed on a slit graphite surface. The results show that there is a preferential adsorption of CO_2 to H_2 in the adsorbed layer, which depends on the temperature. CO_2 adsorbs stronger than H_2 at low temperatures, while at high temperatures there is little preferential adsorption of CO_2 over H_2. The sorption selectivity of CO_2 over H_2 on the graphite surface is invariant to pressure above 25 atm, but reduces when temperature increases. The self-diffusion of CO_2 on graphite surface is the order of magnitude $\sim 10^{-8}$ m^2/s. This is larger than for CO_2 confined in small slit pore by orders of magnitude. The self-diffusion of H_2 on graphite is in very good agreement with available experimental data (Haas et al., 2009). CO_2 has a higher energy barrier of diffusion than H_2. These results of the equilibrium system are useful for process enrichment studies of CO_2.

ACKNOWLEDGMENTS

The authors acknowledge The Research Council of Norway NFR project no 209337 and The Faculty of Natural Science and Technology, Norwegian University of Science and Technology (NTNU) for financial support. The calculation power is granted by The Norwegian Metacenter for Computational Science (NOTUR).

REFERENCES

Allen, M. P., and Tildesley, D. J. (1989). *Computer Simulation of Liquids.* Oxford: Oxford university press.

Bernardo, P., Drioli, E., and Golemme, G. (2009). Membrane gas separation: a review/state of the art. *Ind. Eng. Chem. Res.* 48, 4638–4663. doi: 10.1021/ie8019032

Boukhvalov, D. W., Katsnelson, M. I., and Lichtenstein, A. I. (2008). Hydrogen on graphene: electronic structure, total energy, structural distortions and magnetism from first-principles calculations. *Phys. Rev. B* 77:035427. doi: 10.1103/PhysRevB.77.035427

Cao, D. P., and Wu, J. Z. (2005). Modeling the selectivity of activated carbons for efficient separation of hydrogen and carbon dioxide. *Carbon* 43, 1364–1370. doi: 10.1016/j.carbon.2005.01.004

Essmann, U., Perera, L., Berkowitz, M. L., Darden, T., Lee, H., and Pedersen, L. G. (1995). A smooth particle mesh Ewald method. *J. Chem. Phys.* 103, 8577–8593. doi: 10.1063/1.470117

Goedecker, S., Teter, M., and Hutter, J. (1996). Separable dual-space Gaussian pseudopotentials. *Phys. Rev. B* 54:1703. doi: 10.1103/PhysRevB.54.1703

Grimme, S. (2006). Semiempirical GGA-type density functional constructed with a long-range dispersion correction. *J. Comput. Chem.* 27, 1787–1799. doi: 10.1002/jcc.20495

Guo, B., Chang, L., and Xie, K. (2006). Adsorption of carbon dioxide on activated carbon. *J. Nat. Gas Chem.* 15, 223–229. doi: 10.1016/S1003-9953(06)60030-3

Haas, O.-E., Simon, J. M., and Kjelstrup, S. (2009). Surface self-diffusion and mean displacement of hydrogen on graphite and a PEM fuel cell catalyst support. *J. Phys. Chem. C* 113, 20281–20289. doi: 10.1021/jp902491s

Hartwigsen, C., Gœdecker, S., and Hutter, J. (1998). Relativistic separable dual-space Gaussian pseudopotentials from H to Rn. *Phys. Rev. B* 58:3641. doi: 10.1103/PhysRevB.58.3641

He, X., Arvid Lie, J., Sheridan, E., and Hägg, M.-B. (2009). CO2 capture by hollow fibre carbon membranes: experiments and process simulations. *Energy Proc.* 1, 261–268. doi: 10.1016/j.egypro.2009.01.037

He, X., and Hägg, M.-B. (2011). Hollow fiber carbon membranes: investigations for CO2 capture. *J. Membr. Sci.* 378, 1–9. doi: 10.1016/j.memsci.2010.10.070

He, X., and Hägg, M.-B. (2012). Structural, kinetic and performance characterization of hollow fiber carbon membranes. *J. Membr. Sci.* 390–391, 23–31. doi: 10.1016/j.memsci.2011.10.052

Himeno, S., Komatsu, T., and Fujita, S. (2005). High-pressure adsorption equilibria of methane and carbon dioxide on several activated carbons. *J. Chem. Eng. Data* 50, 369–376. doi: 10.1021/je049786x

http://cp2k.berlios.de (2011). *Branch 2.2 Edn.*

Jin, Y., Lee, D., Lee, S., Moon, W., and Jeon, S. (2011). Gravimetric analysis of CO2 adsorption on activated carbon at various pressures and temperatures using piezoelectric microcantilevers. *Anal. Chem.* 83, 7194–7197. doi: 10.1021/ac201786n

Kim, H. W., Yoon, H. W., Yoon, S.-M., Yoo, B. M., Ahn, B. K., Cho, Y. H., et al. (2013). Selective gas transport through few-layered graphene and graphene oxide membranes. *Science* 342, 91–95. doi: 10.1126/science.1236098

Kjelstrup, S., and Bedeaux, D. (2008). *Non-Equilibrium Thermodynamics of Heterogeneous Systems.* Singapore: World Scientific Singapore.

Levesque, D., and Lamari, F. D. (2009). Pore geometry and isosteric heat: an analysis of carbon dioxide adsorption on activated carbon. *Mol. Phys.* 107, 591–597. doi: 10.1080/00268970902905802

Li, H., Song, Z., Zhang, X., Huang, Y., Li, S., Mao, Y., et al. (2013). Ultrathin, molecular-sieving graphene oxide membranes for selective hydrogen separation. *Science* 342, 95–98. doi: 10.1126/science.1236686

Lim, Y.-I., Bhatia, S. K., Nguyen, T. X., and Nicholson, D. (2010). Prediction of carbon dioxide permeability in carbon slit pores. *J. Membr. Sci.* 355, 186–199. doi: 10.1016/j.memsci.2010.03.030

Lippert, G., Hutter, J., and Parrinello, M. (1997). A hybrid Gaussian and plane wave density functional scheme. *Mol. Phys.* 92, 477–488. doi: 10.1080/00268979770220

Martyna, G. J., Klein, M. L., and Tuckerman, M. (1992). Nosé–Hoover chains: the canonical ensemble via continuous dynamics. *J. Chem. Phys.* 97, 2635. doi: 10.1063/1.463940

Mayo, S. L., Olafson, B. D., and Goddard, W. A. (1990). DREIDING: a generic force field for molecular simulations. *J. Phys. Chem.* 94, 8897–8909. doi: 10.1021/j100389a010

Montoya, A., Mondragón, F., and Truong, T. N. (2003). CO2 adsorption on carbonaceous surfaces: a combined experimental and theoretical study. *Carbon* 41, 29–39. doi: 10.1016/S0008-6223(02)00249-X

Perdew, J. P., Burke, K., and Ernzerhof, M. (1996). Generalized gradient approximation made simple. *Phys. Rev. Lett.* 77, 3865–3868. doi: 10.1103/PhysRevLett.77.3865

Potoff, J. J., and Siepmann, J. I. (2001). Vapor–liquid equilibria of mixtures containing alkanes, carbon dioxide, and nitrogen. *AIChE J.* 47, 1676–1682. doi: 10.1002/aic.690470719

Rostrup-Nielsen, J. R., and Christiansen, L. J. (2011). *Concepts in Syngas Manufacture.* Singapore: World Scientific.

Rubes, M., Kysilka, J., Nachtigall, P., and Bludsky, O. (2010). DFT/CC investigation of physical adsorption on a graphite (0001) surface. *Phys. Chem. Chem. Phys.* 12, 6438–6444. doi: 10.1039/c001155j

Saha, B. B., Jribi, S., Koyama, S., and E-Sharkawy, I. I. (2011). Carbon dioxide adsorption isotherms on activated carbons. *J. Chem. Eng. Data* 56, 1974–1981. doi: 10.1021/je100973t

Sevilla, M., and Fuertes, A. B. (2012). CO2 adsorption by activated templated carbons. *J. Colloid Interface Sci.* 366, 147–154. doi: 10.1016/j.jcis.2011.09.038

Simon, J. M., Haas, O. E., and Kjelstrup, S. (2010). Adsorption and desorption of H2 on graphite by molecular dynamics simulations. *J. Phys. Chem. C* 114, 10212–10220. doi: 10.1021/jp1011022

Smith, W., Yong, C., and Rodger, P. (2002). DL_POLY: application to molecular simulation. *Mol. Simul.* 28, 385–471. doi: 10.1080/08927020290018769

Vandevondele, J., and Hutter, J. (2007). Gaussian basis sets for accurate calculations on molecular systems in gas and condensed phases. *J. Chem. Phys.* 127, 114105. doi: 10.1063/1.2770708

Vandevondele, J., Krack, M., Mohamed, F., Parrinello, M., Chassaing, T., and Hutter, J. (2005). QUICKSTEP: fast and accurate density functional calculations using a mixed Gaussian and plane waves approach. *Comput. Phys. Commun.* 167, 103–128. doi: 10.1016/j.cpc.2004.12.014

Vasanth Kumar, K., and Rodríguez-Reinoso, F. (2012). Effect of pore structure on the selectivity of carbon materials for the separation of CO2/H2 mixtures: new insights from molecular simulation. *RSC Adv.* 2, 9671. doi: 10.1039/c2ra20775c

Zhou, J., and Wang, W. (2000). Adsorption and diffusion of supercritical carbon dioxide in slit pores. *Langmuir* 16, 8063–8070. doi: 10.1021/la000216e

Conflict of Interest Statement: The authors declare that the research was conducted in the absence of any commercial or financial relationships that could be construed as a potential conflict of interest.

Received: 04 September 2013; accepted: 12 December 2013; published online: 24 December 2013.

*Citation: Trinh TT, Vlugt TJH, Hägg M-B, Bedeaux D and Kjelstrup S (2013) Selectivity and self-diffusion of CO_2 and H_2 in a mixture on a graphite surface. Front. Chem. **1**:38. doi: 10.3389/fchem.2013.00038*

This article was submitted to Physical Chemistry and Chemical Physics, a section of the journal Frontiers in Chemistry.